



AERODYNAMIC ANALYSIS OF A VERTICALLY LANDING LIFTING BODY

Selin ARADAĞ*, Jurgen SEIDEL, Russell M. CUMMINGS** and Layne COOK***

*TOBB University of Economics and Technology, Ankara, 06560, Turkey

**United States Air Force Academy, USAF Academy, CO, 80840

***Universal Space Lines LLC, Broomfield, CO, 80020

saradag@etu.edu.tr (corresponding author)

(Geliş Tarihi: 01.08.2011, Kabul Tarihi: 17.04.2014)

Abstract: The vertical landing lifting body (VLLB) is a new concept for reusable launch vehicles, which launches vertically, but re-enters the atmosphere at a high angle of attack (alpha) for its entire flight. The VLLB remains at high angles of attack through all Mach numbers under aerodynamic control until shortly before touchdown. One of the important risk areas for the VLLB concept concerns flight below Mach 2 at high angles of attack where the flow is dominated by separated, highly vortical behavior. The purpose of this study is to investigate the aerodynamic characteristics and control effectiveness of the high-alpha flow of the Hot Eagle Vertically Landing Lifting Body geometry. Several test cases were performed utilizing Detached Eddy Simulations (DES) to both analyze and control the flow over Hot Eagle geometry at different flow conditions. According to results of the time-dependent DES computations, the flow is symmetric and steady at both subsonic and transonic Mach numbers for both 45 and 60 degrees angle of attack. As the angle of attack or the Mach number increases, the vortices get stronger; but the flow remains steady and symmetric. This is probably because of the blunt nature of the nose and its cross-section. Symmetric and asymmetric blowing were performed to control the flow structure around the body. Different blowing rates have been investigated, and the vehicle is found to be controllable with reasonable amounts of blowing.

Keywords: computational fluid dynamics, vertical landing, aerodynamics, flow control, blowing

DIKEY İNİŞ YAPAN BİR ARACIN AERODİNAMİK ANALİZİ

Özet: Dikey iniş, yeniden kullanılabilen roketler için oldukça yeni bir konsepttir. Araçlar dikey olarak atılır, atmosfere yüksek hücum açısıyla girer ve uçuşu boyunca, aerodinamik kontrol altında, yüksek hücum açılarında kalır. İniş çok yakın bir zamana kadar araç, tüm Mach sayıları için yüksek hücum açılarında kalır. Bu konseptle ilgili en önemli risk, Mach 2 altındaki akışlar içindir. Bu Mach sayılarında ve yüksek hücum açılarındaki durumlarda, ayrılmış ve girdaplı akışlar oldukça sık görülür. Bu çalışmanın amacı, yüksek hücum açıları için, dikey iniş yapan Hot Eagle araç geometrisinin aerodinamik özelliklerinin ve kontrol edilebilir stratejilerinin incelenmesidir. Detached Eddy Simulation (DES) yöntemiyle çeşitli test durumları incelenmiş, farklı akış koşulları için araç geometrisinin kontrolü ile ilgili analizler gerçekleştirilmiştir. Zamana bağlı DES sonuçlarına göre, test edilen sesaltı ve transonic Mach sayıları için, 45 ve 60 dercelik hücum açılarında, akış, simetrik ve zamana bağlı değişmeyen akış niteliği göstermektedir. Mach sayısı veya hücum açısı arttıkça, girdaplar güçlenmekte; fakat akışın simetrik ve zamana bağlı değişmeyen tabiatında değişiklik olmamaktadır. Bunun sebebinin aracın uç kısmının küt cisim olma özelliğinden kaynaklandığı düşünülmektedir. Simetrik ve antisimetrik olarak hava üflemenin akış üzerindeki etkileri incelenmiş, çeşitli üfleme hızlarında, akışın kontrol edilebilir olduğu gözlemlenmiştir.

Anahtar kelimeler: hesaplamalı akışkanlar dinamiği, dikey iniş, aerodinamik, akış kontrolü, hava üfleme

NOMENCLATURE

A, N Axial and normal force, lb

Q, R Orthogonal and upper triangular matrixes in QR factorization

A_D Surface area of vehicle, 5518in²

A_{ref} Vehicle reference area, 23756in²

A_s Blowing slot area, 0.75in²

C_A Axial force coefficient

C_l Roll moment coefficient

C_m Pitch moment coefficient

C_N Normal force coefficient

C_n Yaw moment coefficient

C_μ Blowing coefficient

f Frequency, cycles/s

L Body length, 330in

l, m, n Roll, pitch, and yaw moment, in-lb

q_∞ Freestream dynamic pressure, lb/in²

Re Reynolds number

St Strouhal number

U_b Blowing velocity

U_∞ Freestream velocity

x, y, z Axial, lateral, and vertical distances from nose, in

α Angle of attack, deg

β	Angle of sideslip, deg
ρ	Air density, snails/in ³
μ	Dynamics viscosity

INTRODUCTION

The Vertically-Landing Lifting Body (VLLB) is a new concept for reusable launch vehicles (RLV). It launches vertically, but re-enters the atmosphere at a high angle of attack (α) for its entire flight. This distinguishes it from other concepts. While most re-entry vehicles fly at a high angle-of-attack hypersonically, they pitch down to low angles of attack as they slow to supersonic and subsonic speed. The VLLB remains at high angles of attack (between 40 and 80 degrees) through all Mach numbers under aerodynamic control until shortly before touchdown, when the landing engines are started and provide lift and control with thrust, making a powered, vertical landing.

It traces its origins to the McDonnell Douglas X-33 proposal in the early nineties, and is based on that team's experience building and flying the Delta Clipper Experimental (DC-X). The DC-X was a 20-ton vertically landing RLV prototype. The VLLB concept helps solve the problems of rotation for landing attitude since it lands vertically and does not have to rotate. Propellant acquisition, and mass fraction are other advantage of the concept. It has a light enough airframe to reach orbit with a single stage.

It also reduces the sonic boom heard on the ground. Using the all high- α re-entry concept, the VLLB can have a larger payload capacity (or weight margin) than comparable RLV concepts, while enjoying the operational benefits such as no need for rotation to land that come with a powered, vertical landing (Universal Space Lines LLC Final Report, 2006).

It was believed that the blunt, low fineness ratio shape of the VLLB would allow it to have steady, symmetric airflow capable of being modulated to allow yaw moments for directional control. Much research has been conducted in the last twenty years dealing with control of the forebody vortex separation point (Malcolm, 1993). There are several methods that can provide forebody flow control, including mechanical and pneumatic methods. Experiments and numerical investigations have shown that both methods are feasible (Ng and Malcolm, 1991, Malcolm et al, 1989). Forebody tangential slot blowing has been shown to be a candidate for forebody flow control, which is accomplished by blowing a thin sheet of air tangentially to the forebody surface from a slot, as shown in Fig. 1. (Murman et al, 1999) The blowing causes the forebody vortices to change positions in the vicinity of the aircraft and alters the side force and yawing moment.

There are several other studies in literature about flow separation control using simultaneous or continuous blowing and/or suction. For example Gillies (1998) mentions alternate blowing and suction at separation points to damp vortex induced oscillations. Zhdanov *et*

al. (2001) investigated blowing from several locations on the surface of a cylinder computationally. Drag coefficient was slightly decreased. Mathelin et al (2005) experimentally worked on the effects of blowing on the wake of a circular cylinder. Blowing is applied continuously from the surface of a porous cylinder at Reynolds numbers ranging from 3,900 to 14,000. Different injection rates are tested, and it is observed that the boundary layer thickness (BLT) is doubled under an injection rate of 5%. The friction stress is lowered and the viscous drag is decreased.

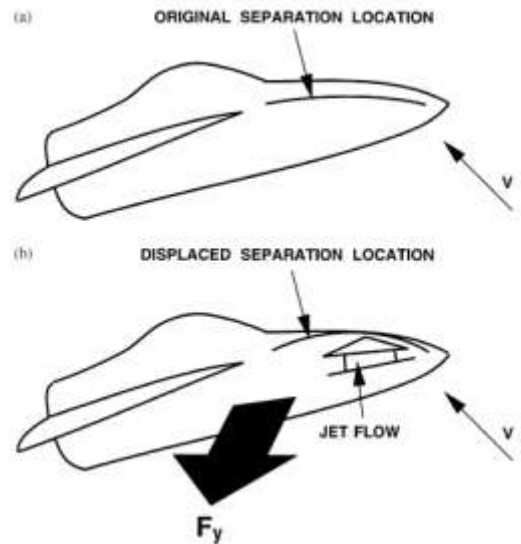


Figure 1. Schematic of pneumatic forebody control concept: a) without blowing, b) with tangential slot blowing (Murman et al, 1999)

Greenblatt and Wygnanski (2000) provide an in depth review on the control of flow separation by periodic excitation. According to Greenblatt and Wygnanski (2000), the first method to be proposed for flow control was suction proposed by Prandtl (1904). Nishri and Wygnanski (1996) showed that separation can be delayed using periodic momentum addition. It is also shown to be effective on airfoil separation by Darabi (2000). There are also other experimental and computational studies in literature that show that blowing and suction can be effective on the control of flow over an airfoil. The location of slots play a crucial role. Wall jet slots were investigated by Seifert and Darabi (1996) and wall-normal slots were investigated by Smith et al (1998).

Separation control was also demonstrated on ramps (Roos and Kegelman, 1986) and on wedges (Zhou et al, 1993). By steady blowing, momentum can directly be added to flow to force it and this can help prevent separation. Carriere and Eichelbrenner (1961) showed applications of steady blowing for flow control. Avoiding the complications of three dimensional effects is important for separation control as demonstrated by Guy et al (1999).

The purpose of this study is to investigate the aerodynamic characteristics and control effectiveness of the high- α flow of the Hot Eagle VLLB geometry

(Fig.2). Several test cases are performed utilizing Computational Fluid Dynamics (CFD) to both analyze and control the flow over Hot Eagle geometry at different flow conditions. Comparisons with available wind tunnel data are also made and the feasibility of using slot blowing for control during re-entry are discussed.

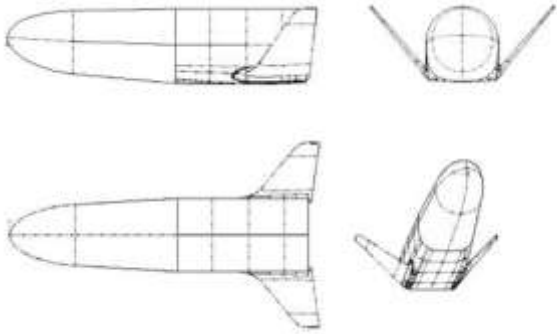


Figure 2. Three-view drawing of Hot Eagle VLLB.

COMPUTATIONAL METHODOLOGY

For the computations, the Cobalt Navier-Stokes solver from Cobalt Solutions, LLC, was used (Strang et al, 1999). It is a commercial code which solves the compressible Navier-Stokes equations using a cell-centered finite volume approach applicable to arbitrary cell topologies (e.g. prisms, tetrahedra). In order to provide second order accuracy in space, the spatial operator uses the exact Riemann solver of Gottlieb and Groth (1988) and least squares gradient calculations using QR factorization. It also utilizes TVD flux limiters to limit extremes at cell faces. A point implicit method using analytic first-order inviscid and viscous Jacobians is used for advancement of the discretized system. A Newton sub iteration scheme is employed for the time accurate computations. The method is second order accurate in time.

The time-dependent computations were performed using the Detached Eddy Simulations (DES) technique which was proposed by Spalart et al. (1997) The technique calls upon both Large Eddy Simulation (LES) and Reynolds Averaged Navier Stokes (RANS) turbulence modeling, to develop a numerically feasible and accurate approach combining the most favorable elements of each. DES can be viewed as a modification of Reynolds Averaged Navier Stokes Equations (RANS). It uses Large Eddy Simulations (LES) by using subgrid scale formulation where the turbulent length scale is large enough to use LES, ie: where the turbulent length scale is larger than grid dimensions. For the solutions near solid boundaries where turbulence scale is comparable to grid size, RANS is used. With this, DES does not have to use RANS for regions fine enough for LES, therefore the cost of the computation is cut down.

The primary advantage of DES is that it can be applied at high Reynolds numbers (as can Reynolds averaged techniques), and it resolves geometry-dependent, unsteady three-dimensional turbulent motions as in LES.

The unstructured finite volume solver Cobalt (Strang et al, 1999) has been used in conjunction with DES successfully on a number of complex problems, including a supersonic base flow (Forsythe et al, 2002), the F-15E (Forsythe et al, 2002) at high angle of attack and the F-18C (Morton et al, 2003).

The grid is an unstructured grid generated by Gridtool/VGRID using the method of Morton et al. (2002) The grid has 10 million cells with point clustering at the wall of $y^+_{\text{average}} < 0.3$. The modified Riemann invariant condition was selected as a farfield boundary, whereas a no slip, adiabatic wall boundary condition was employed for the body surface.

To make the flow solution at every time step converge, 3 Newton subiterations were used. Time dependent computations were performed for at least 10 flow through times for each case, where one flow through time is defined as the ratio of length of the vehicle to freestream velocity (L/U_∞). The CFD cases investigated are shown in Table 1. Both steady and time-dependent computations were performed in order to investigate the effects of Mach number, angle of attack (α), angle of side slip (β) on the flow as well as the unsteadiness and symmetry of the flow structure.

It is computationally very difficult to start with a uniform flow condition (as an initial condition) and make the transonic and supersonic cases converge. Therefore, in order to be able to perform the simulations for transonic Mach numbers, the results of previous computations were used as an initial condition for the steady computations. The last three cases are flow control cases, where blowing was applied through blowing slots on the surface in order to observe the effects of flow control on steadiness and symmetry of flow of Case 2. Case 9 employs symmetric blowing on both sides, whereas Case 10 and 11 employ asymmetric blowing with a slot only on one side of the geometry.

RESULTS AND DISCUSSION

The results of the computations are presented in two sections. The first section describes the simulated flow structure around the Hot Eagle VLLB, exploring the symmetric and time-dependent behavior of the flow. The next section describes the results of symmetric and asymmetric blowing, and the effects of blowing on the flow structure.

Analysis of Flow Structure

Fig 3 shows the instantaneous contours of x-vorticity for the first eight test cases at $x = 100\text{in}$ where x is defined starting from the nose along the body axis. As seen in Fig. 3, the vortex structure changes and the vortices get stronger as the Mach number and angle of attack increases. Except for Case 4, where $\beta = 5^\circ$, all cases show a symmetric vortex structure, because of the blunt nature of the nose.

Table 1. Computational fluid dynamics test cases

Case	Altitude (ft)	Mach number	Pressure (psi)	Temperature (R)	α (deg)	β (deg)	Control
1	30,000	0.3	4.3641	411.69	45	0	No
2	75,000	0.7	0.5073	395.12	45	0	No
3	75,000	0.7	0.5073	395.12	60	0	No
4	75,000	0.7	0.5073	395.12	45	5	No
5	90,000	0.9	0.251	403.35	45	0	No
6	95,000	1.0	0.199	406.1	45	0	No
7	105,000	1.1	0.1258	411.6	45	0	No
8	110,000	1.2	0.1	419.0	45	0	No
9	75,000	0.7	0.5073	395.12	45	0	Symmetric blowing
10	75,000	0.7	0.5073	395.12	45	0	Asymmetric blowing
11	75,000	0.7	0.5073	395.12	45	0	Asymmetric blowing increased blow rate

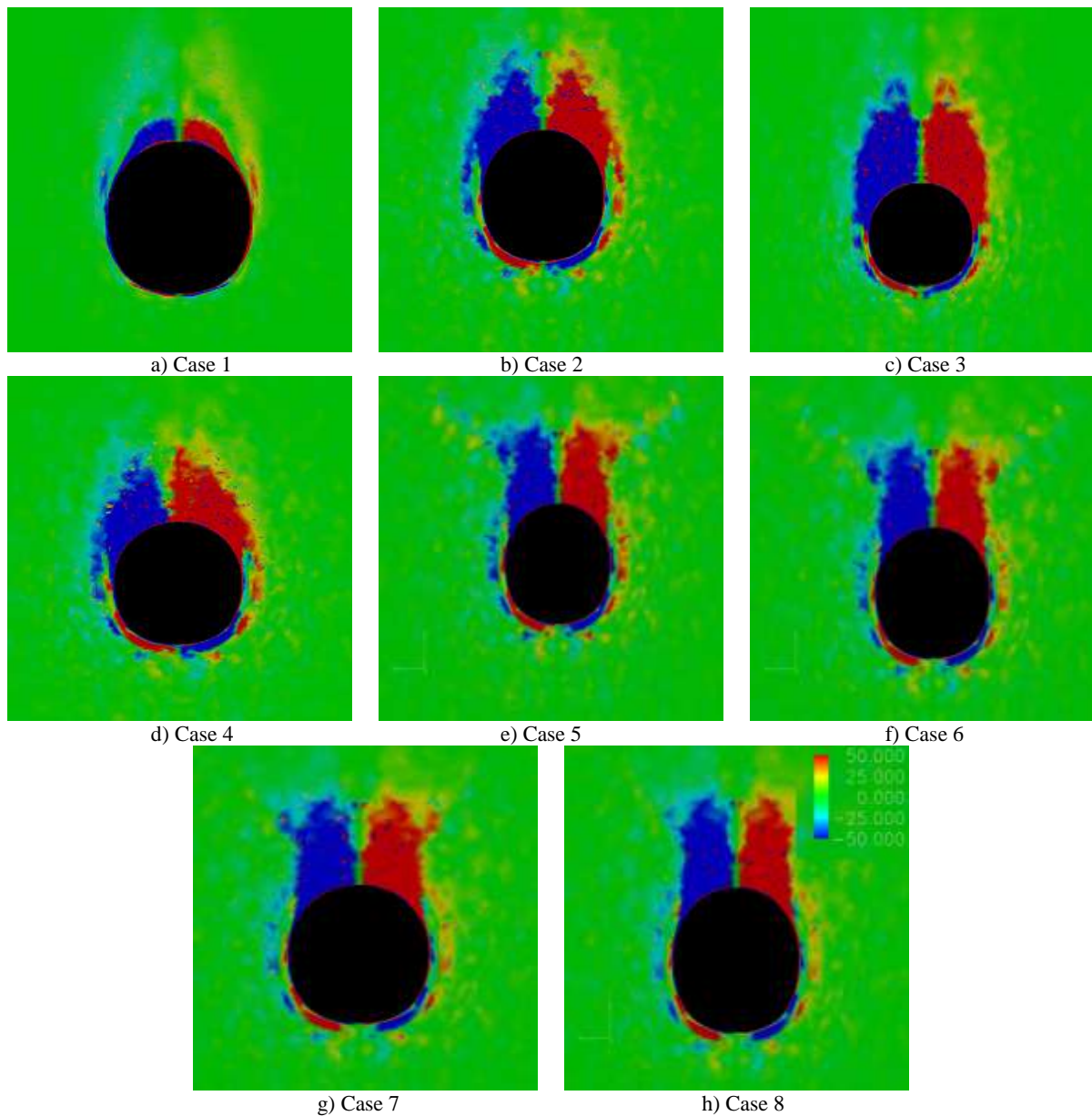


Figure 3. X-vorticity contours at $x = 100in$.

Time histories of the forces in x, y, and z-directions are shown in Fig. 4 for the simulation at Mach 0.3 (Case 1) as a representative solution (the same trends are observed

in the other cases). There are fluctuations in all three forces which show unsteadiness in the computational results. However, excitingly, when the time-dependent

flow structure on the forebody ($x = 100\text{in}$) is examined in terms of x -vorticity, by taking two time values which are supposed to show different structures because they have different z -forces as shown in Fig. 4, such as $t = 0.60\text{s}$ and $t = 0.65\text{s}$, it is seen in Fig. 5 that the vortex structure at $x = 100\text{in}$ is not different for these two time values. This shows that there is no unsteadiness on the forebody portion of the vehicle. On the other hand, Fig. 6 shows the y -vorticity contours at the centerplane of the body ($y = 0\text{in}$) at these two time values. As seen in Fig. 6, the reason for the fluctuations of forces in Fig. 4 is the wake behind the body, which is highly unsteady in nature with vortex shedding taking place. Specifically, a power spectrum density analysis of the force in the z -direction shows that the primary frequency of unsteadiness has a Strouhal number of $St=0.28$, which corresponds to blunt body vortex shedding in a base region, as seen in Fig. 6. (Schiavetta et al, 2007)

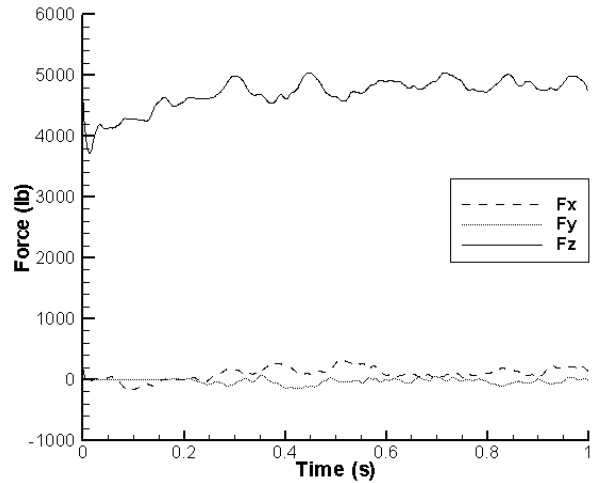


Figure 4. Time history of forces for Case 1.

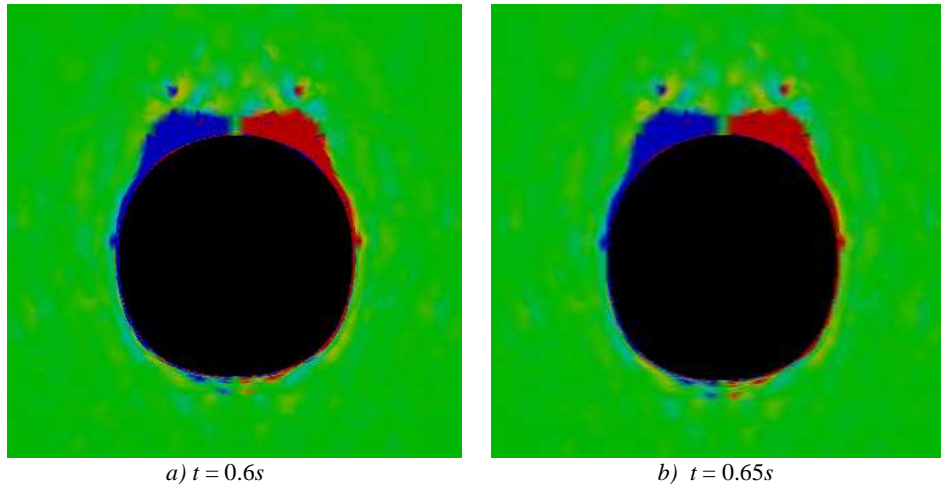


Figure 5. Instantaneous x -vorticity contours at $x = 100\text{in}$.

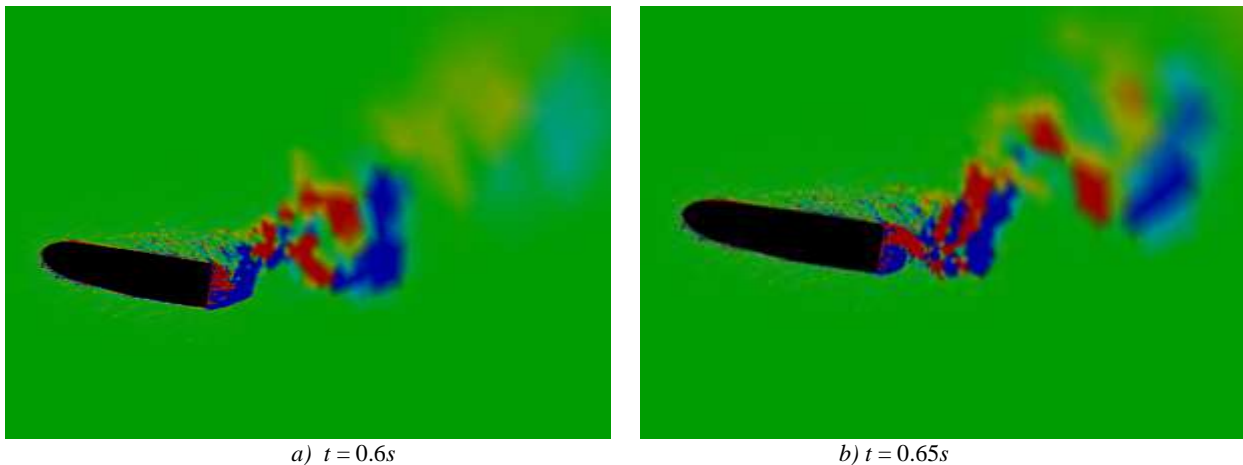


Figure 6. Instantaneous y -vorticity contours at $y = 0\text{in}$ (vehicle centerline).

Table 2 shows the normal and axial force coefficients extracted from the computational results for the test cases and the coefficients obtained by Turri (2006) from wind tunnel measurements. Turri (2006) performed wind tunnel experiments and measured normal and axial coefficients for the flow at the same Mach number, \square , and \square as Case 1. The moment coefficients, calculated using the vehicle length (330in) as the reference length,

are shown in Table 2 as well. Although the wind tunnel experiments were performed at different Reynolds numbers, comparison of the coefficients can give a rough idea about the validity of the computational results of Case 1. Additionally, the wind tunnel model included extended body flaps, while the CFD model did not, which should have an impact on the normal force and pitch moment coefficients.

Control Effectiveness of Symmetric and Asymmetric Blowing

The effects of blowing on the flow structure over the Hot Eagle geometry was investigated by utilizing both symmetric and asymmetric blowing. The grid generated for the computations is shown in Fig. 7.

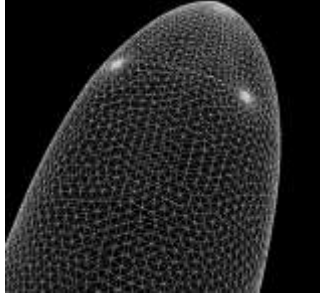


Figure 7. Grid for blowing slots

The grid has blowing slots on both sides to enable mass flow out of the blowing slots, thereby controlling the flow for the solution of these three cases. The blowing slots were located at the position where the separation from the surface started. The blowing velocity was set to 10% of the freestream velocity of 8185in/s. The ratio of the blowing area to total surface area is 0.00014, where the blowing area is 0.75in² and the total surface area is 5518in². The

mass flow rate through the blowing slot is calculated to be 3.19×10^{-6} snails/s for Cases 9 and 10. For case 11, the asymmetric blowing rate was increased to five times this rate (1.6×10^{-5} snails/s), which is 50% of the freestream velocity. As a boundary condition for the blowing slots, a source boundary condition was specified with the calculated mass flow. The non-dimensional blowing coefficient (C_μ) is defined as:

$$C_\mu = \frac{\rho U_b^2 A_s}{\rho U_\infty^2 A_D} = 1.36 \times 10^{-6} \quad (1)$$

For the computations of Cases 10 and 11 (asymmetric blowing), the symmetric grid generated for Case 9 (symmetric blowing) was used, by specifying a solid wall boundary condition on one side and blowing on the other side. Figure 8 shows surface pressure contours of symmetric blowing with slots on both sides and Fig. 9 shows asymmetric blowing with a slot on one side, only. As seen in Figs. 8 and 9, there is no visual change in surface pressures when the blowing slot on one side is not activated; and neither asymmetric nor symmetric blowing change the flow structure before blowing. There are several possible reasons for this result. Amount of blowing, location of blowing slots, stability and steadiness of the flow are the most important of these reasons.

Table 2. Normal force, axial force, and moment coefficients

Case	Re	C_N	C_A	C_m	C_n	C_ℓ
1 Computation	23.4 M	0.762	0.045	-0.422	-0.0002	-0.0002
1 Experiment (Turri, 2006)	4.3 M	0.897	-0.169	-	-	-
2 Computation	6.7 M	0.942	0.006	-0.497	-0.012	-0.0005
3 Computation	6.7 M	1.234	-0.054	-0.620	0.023	0.00006
4 Computation	6.7 M	0.933	0.008	-0.478	-0.11	0.005
8 Computation	2.1 M	0.971	0.085	-0.523	-0.00001	-0.000003

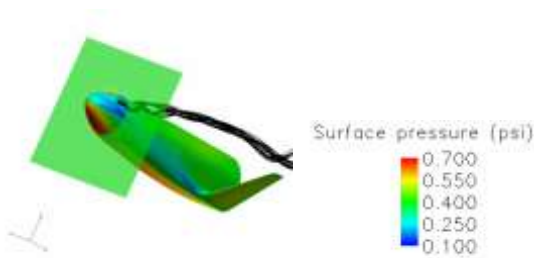


Figure 8. Pressure contours and x -vorticity for symmetric blowing.

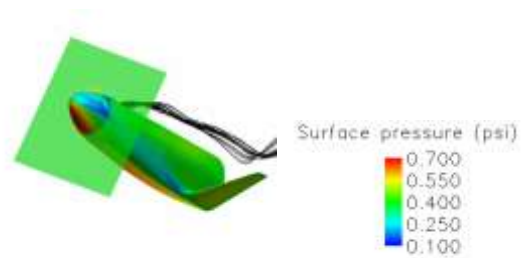


Figure 9. Pressure contours and x -vorticity for asymmetric blowing.

Table 3. Normal, axial force, and moment coefficients for blowing cases.

Case	C_N	C_A	C_m	C_n	C_ℓ
2 No Blowing	0.942	0.006	-0.497	-0.012	-0.0005
9 Symmetric Blowing	0.995	0.026	-0.523	0.004	-0.0024
10 Asymmetric Blowing	0.998	0.004	-0.523	0.012	0.0024
11 Asymmetric blowing with increased blow rate	0.982	0.010	-0.506	-0.013	0.0005

Although, there is no change in the flow structure, the normal and axial force and moment coefficients extracted from the computational results for the blowing cases are

different than the original case without control (Case 2) as shown in Table 3. As seen in Table 3, both symmetric and asymmetric blowing increase the lift coefficient. As

the rate of asymmetric blowing increases the lift coefficient starts dropping but still higher than the original. Asymmetric blowing, only if the blowing rate is high enough can increase the drag coefficient, whereas symmetric blowing clearly increases it. Pitching moment stays approximately constant independent of symmetric and asymmetric blowing and the rate of blowing, whereas roll and yaw moments clearly change with blowing.

These results correspond to the findings of Agosta-Greenman, et al (1995). They found that slot blowing on a forebody could create a variety of results depending on the mass flow rate, with the impact on yaw moment falling into three categories (Fig. 10): Region I (low blowing), Region II (medium blowing), and Region III (high blowing). For Region I (low blowing), the jet causes the primary vortex on the blowing side to move away from the surface and the strength of the vortex is reduced. At the same time, the nonblowing-side vortex moves towards the surface, producing a small side force and yawing moment toward the nonblowing side of the body. For Region II (medium blowing), the primary vortex on the blowing side is entrained by the jet and moves downward towards the surface due to the Coanda effect. The nonblowing-side vortex moves away from the surface. Here, the movement of the vortices and the resulting lower pressure region on the blowing side cause a side force and yawing moment toward the blowing side. This represents a reversal in yaw moment when compared with Region I. At the highest blowing levels for Region III, the jet is so strong that it acts to separate, rather than entrain, the blowing-side vortex flow. The blowing-side vortex moves away from the surface and the nonblowing-side vortex moves toward the surface. This causes the local yaw moment to be negative in the region of the jet. At this high mass flow rate, the pressure at the jet exit is about 10 times greater than the freestream pressure. Hence, the jet rapidly expands after leaving the blowing slot, which causes the jet to separate, and pushes the primary vortex away from the surface. The results in Table 3 appear to validate this description, as the low blowing case (Case 10) resulted in a reversal of the yaw moment, while the higher blowing case (Case 11) had a similar yaw moment to the no blowing case (Case 2). This yields a control mechanism that can create a variety of yaw moments depending on the amount of blowing used and the choice of which side of the forebody to blow from.

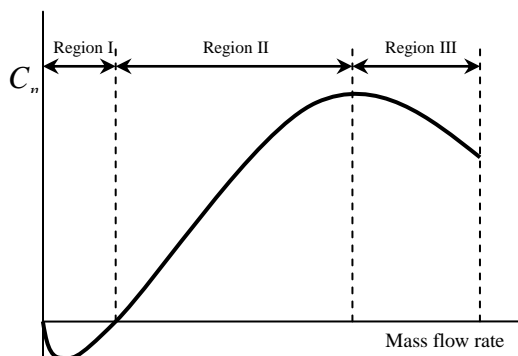


Figure 10. Asymmetric forebody slot blowing impact on yaw moment (Agosta-Greenman et al, 1995)

CONCLUSION AND RECOMMENDATIONS

Detached Eddy Simulation (DES) was applied to perform an investigation of the unsteadiness and asymmetry in the flow structure around the RLV forebody. According to results of the time-dependent DES computations, the flow is symmetric and steady at both subsonic Mach numbers of 0.3, 0.7, 0.9 for both 45 and 60 degrees angle of attack and transonic, supersonic Mach numbers of 1.0, 1.1 and 1.2. As the angle of attack or the Mach number increases, the vortices get stronger; but the flow remains steady and symmetric. This is probably because of the blunt nature of the nose and its cross-section.

Symmetric and asymmetric blowing were performed to control the flow structure around the Hot Eagle Vertical Landing Lifting Body. Symmetric blowing does not change the steady and symmetric nature of the flow structure, as expected. It increases the drag and lift coefficients, whereas it does not have any significant effect on pitching moment.

Asymmetric blowing was performed at two different mass flow rates. Blowing with the lower rate increases the lift coefficient more than blowing with the higher rate, whereas blowing at a higher rate increases the drag coefficient more. This clearly shows that increasing the rate of asymmetric blowing does not affect the force coefficients in a positive way. Although pitching moment does not change significantly with asymmetric blowing, yaw and roll moments are effected.

Asymmetric blowing does not change the steadiness and symmetry of flow. There are several possible reasons for this result. Amount of blowing, location of blowing slots, stability of the flow are the most important of these reasons. Optimization of the location of blowing slots and investigating higher blowing rates for asymmetric blowing are two studies that can be performed in the future.

ACKNOWLEDGMENTS

This research was supported by Universal Space Lines LLC, monitored by Mike Talbot and Mike Mahoney. Funding for the work came from AFRL under the sponsorship of Jess Sponable. The authors would also like to thank to Dr. Dave McDaniel for his help in creating the grid for asymmetric blowing. The results of this study were presented at an AIAA conference.

REFERENCES

- Agosta-Greenman, R M, Gee K, Cummings R M., Schiff L B (1995). Computational Investigation of Tangential Slot Blowing on a Generic Chined Forebody. *Journal of Aircraft*, 32 (4): 811-817.
- Carriere, P., Eichelbrenner, E. A., "Theory of Flow Reattachment by a tangential jet discharging against a strong pressure gradient", Boundary layer and flow

- control: Its principles and applications, 1, Pergamon Press, New York, 1961.
- Darabi, A., "On the Mechanism of Forced Flow Reattachment, PhD Thesis, Tel Aviv University, 2000.
- Forsythe J R, Hoffmann, K A, Cummings R M, Squires K D (2002). Detached-Eddy Simulation with Compressibility Corrections Applied to a Supersonic Axisymmetric Base. *Journal of Fluids Engineering*. 124 (4): 911-923.
- Forsythe J R, Squires K D, Wurtzler K E, Spalart P R (2002). Detached Eddy Simulations of Fighter Aircraft at High Alpha. AIAA Paper 2002-0591.
- Gad-el-Hak, M., *Flow Control; Passive, Active and Reactive Flow Management*, Cambridge University Press, 2000.
- Gottlieb J J, Groth C P T (1988). Assessment of Riemann Solvers for Unsteady One-Dimensional Inviscid Flows of Perfect Gases. *Journal of Computational Physics*. 78 (2): 437-458.
- Greenblatt, D., Wygnanski, I. J., "The Control of Flow Separation by Periodic Excitation", *Progress in Aerospace Sciences*, 36 (7), 487-545, 2000.
- Guy, Y., Morrow, J., McLaughlin, T., "Pressure Measurement and Flowfield Visualization on a Delta Wing with Periodic Blowing and Suction", AIAA Paper-99-4178, 1999.
- Malcolm G N, Ng T T, Lewis L (1989). Development of Non-Conventional Control Methods for High Angle of Attack Flight Using Vortex Manipulators. AIAA Paper 89-2192.
- Malcolm S (1993). Forebody Vortex Control – A Progress Review. AIAA Paper 93-3540.
- Mathelin, L., Bataille, F., Lallemand, A., Near Wake of a Circular Cylinder Submitted to Blowing – I Boundary Layers Evolution, *International Journal of Heat and Mass Transfer* 44, 3701-3708, 2005.
- Morton S A, Forsythe J R, Squires K D, Wurtzler K E (2002). Assessment of Unstructured Grids for Detached Eddy Simulation of High Reynolds Number Separated Flows. Proceedings of the Eight International Conference on Numerical Grid Generation in Computational Field Simulations.
- Morton S A, Steenman M B, Cummings R M, Forsythe J R (2003). DES Grid Resolution Issues for Vortical Flows on a Delta Wing and an F-18C. AIAA Paper 2003-1103.
- Murman S M, Rizk Y M, Cummings, R M, Schiff L B (1999). Computational Investigation of Slot Blowing for Fuselage Forebody Flow Control. *Aircraft Design*, 2 (1): 45-63.
- Nishri, B., Wygnanski, I. , "On flow separation and its control", *Computational Methods in Applied Sciences*, Wiley, New York, 1996.
- Ng T T, Malcolm G N (1991). Aerodynamic Control Using Forebody Strakes. AIAA Paper 91-618.
- Prandtl, L. "Über Flüssigkeitsbewegung bei sehr kleiner-Reibung.", *Proceedings of Third International Mathematical Congress, Heidelberg*, 1904.
- Roos, F. W., Kegelman, J. T., "Control of Coherent Structures in Reattaching Laminar and Turbulent Shear Layers, AIAA Journal, 24 (12), 1956-63, 1986.
- Schiavetta L A, Badcock K J, Cummings R M (2007). Comparison of DES and URANS for Unsteady Vortical Flows over Delta Wings. AIAA Paper 2007-1085.
- Seifert, A., Darabi, A., Wygnanski, I., "Delay of Airfoil Stall by periodic excitation", *AIAA J Aircraft*, 33 (4), 691-698, 1996.
- Spalart P R, Jou W H, Strelets M, Allmaras S R (1997). Comments on the Feasibility of LES for Wings, and on a Hybrid RANS/LES Approach, *Advances in DNS/LES*. 1st AFOSR International Conference on DNS/LES. Greyden Press, Columbus, OH.
- Smith, D., Amitay, M., Kibens, V., Parekh, D., Glezer, A., "Modification of Lifting Body Aerodynamics using Synthetic Jet Actuators", AIAA Paper 98-0209, 1998.
- Strang W Z, Tomaro R F, Grismer M J (1999). The Defining Methods of Cobalt₆₀: A Parallel, Implicit, Unstructured Euler/Navier Stokes Flow Solver. AIAA Paper 99-0786.
- Turri A (2006). High Alpha RLV Aerodynamic Configuration Development. Technical report. Air Vehicles Directorate, Air Force Research Laboratory.
- Universal Space Lines LLC Final Report (2006). The Vertically-Landing Lifting Body (VLLB) Concept for a Reusable Upper Stage. Contract No. RSC05019, AFRL.
- Zhdanov, V. L., Isaev, S. A, Niemann, H. J., Control of the Near Wake of a Circular Cylinder in Blowing Out of Low-Head Jets, *Journal of Engineering Physics and Thermophysics* 74(5), 1100-1103, 2001.
- Zhou, M. D., Fernholz, H. H., Ma, H. Y., Wu, J. Z., Wu, J. M., "Vortex capture by a two dimensional airfoil with a small oscillating leading-edge flap", AIAA paper-93-3266, 1993.